WAVE DIFFRACTION AND TRANSMISSION BY A SUBMERGED BREAKWATER

Filianoti P.[1], Gurnari L.[1]

The wave field around a rectangular submerged breakwater is investigated by means of an experiment in numerical wave flume. The results were compared with those obtained making use of the Boundary Element Method. The numerical experiment is carried out to determine the share of the incident wave energy that are reflected, dissipated over the roof of the breakwater, and transmitted in the lee. The wave field before the breakwater (i.e. the quasi standing field) obtained with the CFD simulations is quite similar to that obtained with the BEM. Some relevant differences between the two models arise in the lee of the breakwater, because the wave motion is strongly affected by the dissipation occuring over the breakwater roof by friction and wave breaking. They cannot be foreseen with BEM, being the motion ideal. Their analysis show that the dissipation is more than halves the transmission of energy, despite the relevant submergence of the considerated breakwater.

Keywords: submerged breakwater; wave diffraction; transmission coefficient; CFD simulation; reflected waves.

INTRODUCTION

Detached breakwaters for coast defense are usually realized by means of rock stones or concrete blocks. These structures rest on the seabed with the crest rising above the mean sea level or remaining below it. Emerged breakwaters do not present wave transmission over the structure, whilst overtopping and significant wave transmission occurs across low-crested breakwaters. Fully submerged breakwaters are employed to minimize the visual intrusion of the breakwater, that is important for recreational coastal developments. In this case, waves pass over the crest of the breakwater with breaking, and higher energy is transmitted in the lee of submerged breakwaters in respect of semi-submerged structures.

The effectiveness of a breakwater in attenuating wave energy can be measured by the amount of wave energy passing the structure. The transmission factor T^2, defined as the ratio between the mean wave energy flux transmitted on the landward side of the structure and the mean wave energy flux of the incident waves on the seaward side of the structure, allows evaluating the effectiveness of the submerged breakwater. In particular, high values of T^2 indicate a small wave attenuation. Empirical formulas, for estimating wave transmission over submerged breakwaters, have been proposed by Harens (1987), d'Angremond et al (1996), Seabrook & Hall (1998).

It is possible to reduce the transmission factor T^2 assuming an "active defense" of the coast. The REsonant Wave Energy Converter (REWEC) is a device useful for this purpose (Boccotti, 2003; Boccotti et al, 2007; Arena & Filianoti, 2007). The first realization of this device (named REWEC1) consists of several caissons in reinforced concrete placed side by side to form a barrier that remains a few meters below the still water level. Each caisson embodies a device for the energy absorption, which exploits the resonance between incident waves and the water motion in the ducts recovered inside the caisson. A worth solution is using the breakwater in two different operational regimes: one for winter seasons, the other for summer seasons. In winter, when generally occur the strongest sea storms, we fill of water the plenum, so the structure operates as a conventional "non-active" submerged breakwater. In this configuration the REWEC1 has a bigger weight, and it is able to better withstand the action of the highest waves. In summer, when the sea storm is generally less severe, and we need more protection in the lee of the breakwater, because sports craft could be moored behind it, we pump air in the plenum, giving the REWEC1 the ability to reduce the energy of waves past over, by partially absorbing it. The performances of these caisson breakwaters have been investigated by Filianoti & Piscopo, (2015). In particular, they propose a semi-analytical model to estimate the wave energy transmitted in the lee of the breakwater, taking in account the energy reflected towards the open sea by the breakwater, the energy absorbed inside it, and the energy dissipated over its roof.

In this work we analyze the wave field around the REWEC1 devices described by Filianoti & Piscopo, (2015) when it works as a conventional "non-active" submerged breakwater. To this aim we carried out numerical simulations using two diffent approaches: the BEM and the CFD, in order to investigate the limits of the first to adeguately represent the wave field arround the submerged breakwater.

[1]University Mediterranea of Reggio Calabria, DICEAM department Via Graziella Feo di Vito, Reggio Calabria,89122, Italy

THE BEM MODEL

We can represent the velocity potential $\mathbf{\Phi}$, in a generic point (y,z) of the flow field, as a sum of the complex incident waves potential $\mathbf{\Phi}_W$, and the diffracted waves potential $\mathbf{\Phi}_S$. Supposing waves are periodic with height H and period T, as the flow is harmonic in the time, the velocity potential can be written in the form

$$\mathbf{\Phi}(x,y,t) = g\frac{H}{2}\omega^{-1}\left[\mathbf{\Phi}_W(y,z) + \mathbf{\Phi}_S(y,z)\right] exp(-i\omega t). \tag{1}$$

The term due to the incident waves is known:

$$\mathbf{\Phi}_W(y,z) = -i\frac{\cosh[k(d+z)]}{\cosh(kd)} exp(-iky). \tag{2}$$

The term due to the diffracted waves is obtained supposing a uniform distribution of wave sources on the contour of the submerged body, each of them with a different intensity. It can be expressed as an integral equation (Wehausen & Laitone, 1960):

$$\mathbf{\Phi}_S(y,z) = \frac{1}{2\pi}\int_\Gamma f(\eta,\zeta)\mathbf{G}(y,z;\eta,\zeta)d\Gamma, \tag{3}$$

where f is the source intensity function, $\mathbf{G}$ is Green's function related to a punctual source of unit intensity placed in the point (η, ζ) on the submerged contour Γ of the structure.

Green's function is known, but the sources intensity doesn't. The source function $\mathbf{G}$ in two dimension was given by Wehausen & Laitone (1960). To compute $f(\eta,\zeta)$, we assign the normal velocity on the structure contour to be equal to zero on the same contour:

$$-\frac{1}{2}f(x,y) + \frac{1}{4\pi}\int_l f'(\xi,\eta)\frac{\mathbf{G}(x,y;\xi,\eta)}{\partial n}dl = -\frac{1}{k}\frac{\partial\phi_i}{\partial n}. \tag{4}$$

Since we are not able to solve Eq. (4) analytically, we recurr to a numerical approach, generally known as boundary element method (BEM). For numerical solution, Eq. (4) is replaced by a sequence of algebraic equation, obteined subdividing the submerged contour of the structure in a finite number of segments, each of them characterized by the size, the barycentre coordinate and the direction cosines of the normal pointed outward the body contour. So, the position of each source is identified by the barycentre position of each element, in accordance with the geometric scheme represented in Fig.1.

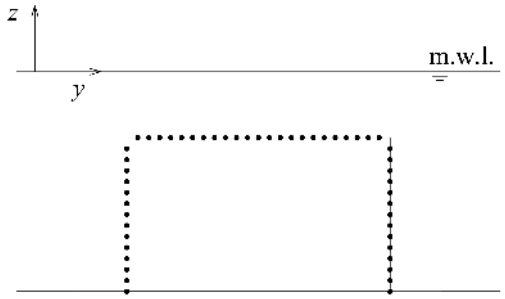

Figure 1: Reference scheme of the structure. Points represent the position of sources located on the body contour.

We define respectively $\tilde{\mathbf{G}}$ as the real part and $\tilde{\mathbf{F}}$ as the imaginary part of $\mathbf{\Phi}_W + \mathbf{\Phi}_S$. So, that Eq. (1) can be rewritten in the form

$$\mathbf{\Phi}(y,z,t) = g\frac{H}{2}\omega^{-1}\left\{[\tilde{\mathbf{G}}(y,z)\cos(\omega t) + \tilde{\mathbf{F}}(y,z)\sin(\omega t)] + i[\mathbf{G}(y,z)\sin(\omega t) + \mathbf{F}(y,z)\cos(\omega t)]\right\}. \tag{5}$$

The physical meaning of Eq. (5) is attribuited to its real part.

RESULTS OF THE BEM ANALYSIS

Whenever a wave train attacks a piercing vertical wall, we assist to a phenomenon known as reflection. The reflected wave train superimposes with the incident waves generating a standing wave field in front of the breakwater wall. This is characterized by the presence of 'nodes', which are points where the free surface elevation is always zero, and 'antinodes', where the free surface elevation are maxima (both positive and negative). In this wave field there is no energy transfer from one place to another. This phenomenon appears when two progressive waves with the same frequency and amplitudes, travelling in opposite directions, superimpose in opposite phases. The resulting wave field obtained by the interaction between the progressive wave train and the submerged breakwater is a quasi-standing field, characterized by the presence of 'pseudo-antinodes' and 'pseudo-nodes'. The latters denote the energy transferring in the lee of the breakwater. Fig. 2 shows the envelope of the free surface displacement forming a quasi-standing field.

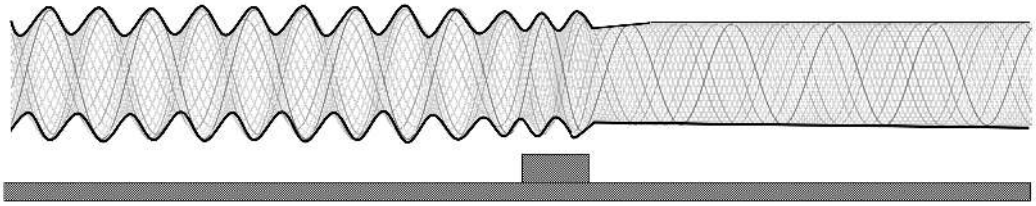

Figure 2: Envelope of free surface displacement around the submerged breakwater.

The wave reflection in front of a submerged breakwater is partial, because a share of the incident energy is trasmitted in the lee of the breakwater. The reflection coefficient R (and transmission coefficient T), represents the ratio between the reflected wave height (transmitted wave height) and the incident wave height. R and T was evaluated as suggested by Chakrabarti, (1994), and are equal to 0.256 and 0.96 respectively. The Healy's (1952) formula to evaluate R, gives:

$$R = \frac{H_v - Hn}{H_v + H_n}, \tag{6}$$

where H_v and H_n (see Fig. 3) are the quasi-antinode and the quasi-node height, respectively. They are equal to 2.5 m and to 1.46 m, respectively, giving $R = 0.26$, in perfect agreement with the value obtained through the BEM formulas (Chakrabarti, 1994). This allows us to utilize Eq.(6) in the next section to evaluate R.

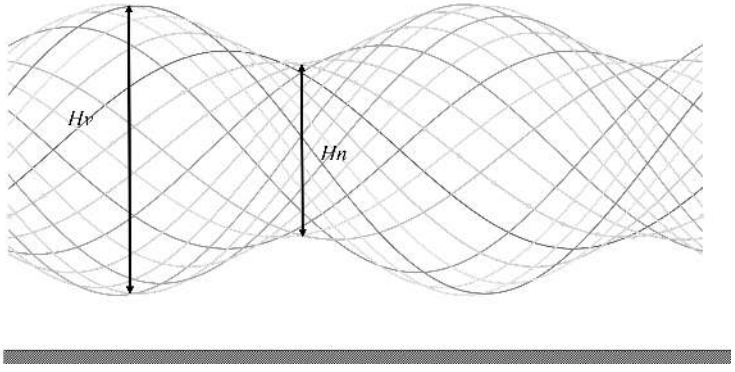

Figure 3: Particular of the envelope shown in Fig. 2.

THE CFD MODEL

Layout and model of the numerical experiment

In order to analyse the wave field around the submerged breakwater, we carried out an experiment in a numerical wave flume equipped by a piston type wavemaker. The wave flume is 1 km long and the

submerged breakwater is placed at the middle of the domain. As shown in Fig. 4, the water depth is 10 m and the structure is 22.5 m long and 7 m high (Filianoti & Piscopo, 2015). The length of the numerical flume has been chosen in order to have many wave lengths in front of and behind the submerged breakwater, where stationary condition are well established.

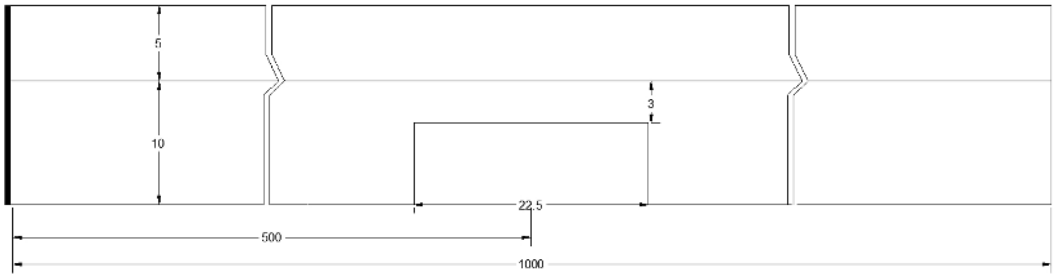

Figure 4: Sketch of the computational domain.

The numerical approach is based on a two-dimensional CFD simulation using the Euler-Euler approach, implemented in the commercial code Ansys Fluent 17.0, Academic Version. To represent the air-water interface we used the volume of fluid (VOF) model in which two or more fluids (or phases) are not interpenetrating between each other. In order to obtain the spatial discretization of the convection terms in the governing equations, we used the Green-Gauss Cell-Based method to gradient evaluation and the PRESTO! (PREssure STaggering Option) scheme for pressure equation. The other convection-diffusion equations (e.g. momentum or energy equation) were discretised by means of the Second Order Upwind scheme. In this work, we use the all "triangles mesh" method, exept near the air-water interface, where the mesh adopted is rectangular. This choice is made to achieve a better resolution of the instantaneous free surface displacement. The size of mesh is variable according to geometrical needs. In particular, we adopted a ticker mesh near the structure edges than elsewhere in the domain. In order to match the behavior of a physical wave flume, we have to set smooth no-slip wall boundary conditions to all solid walls, whilst the upper domain boundary is defined as a pressure outlet with zero-gauge pressure. The wave-flume has a piston-type wavemaker placed on the left extremity of the computational domain. Starting from rest, the wave generation process has been simulated assigning a sinusoidal velocity to the left wall of the wave flume, by means of a User Defined Function (UDF). The Fluent dynamic mesh feature has been used for both the wall motion and the deformation of the neighboring cells. The wave field generated is characterized by 4.8 s of wave period T, and 1.5m of wave height H.

The wave field in front of and behind the breakwater

Fig. 5 shows the envelope of the surface displacement in front of the breakwater, obtained overlapping several snapshots taken every 1/20 of the wave period T. As we can see, the successive wave profiles form the typical envelope of a progressive wave train, propagating in a flume initially at rest. The wave height is practically constant in the tail of the wave train (near the wavemaker) and it reduces gradually to zero at the head of the wave train.

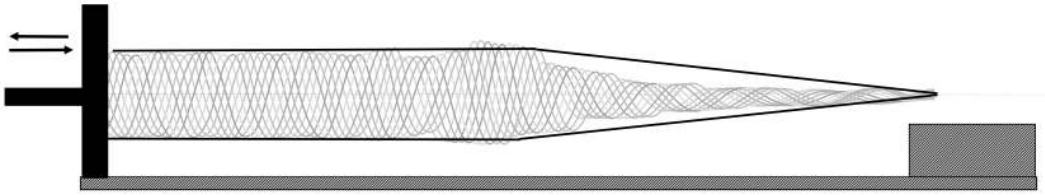

Figure 5: The progressive wave field propagating towards the submerged breakwater, in the flume initially at rest.

Moreover, we can appreciate the expansion of the quasi-standing wave field towards the wavemaker. Indeed, Fig. 6 shows the envelope of the free surface after the wave train have impacted the submerged

barrier. As we can see, in front of the structure the wave field is the superimposition of two wave train: the incoming and the reflected one. The sum produces a quasi standing field which expands towards the wavemaker. The arrow shows the transition between the incoming waves and the quasi stationary waves.

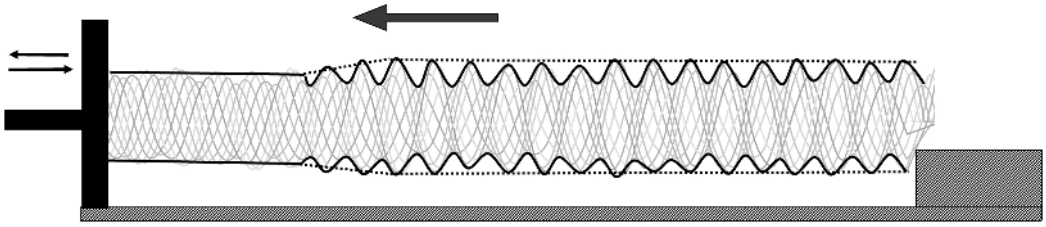

Figure 6: The superimposition of two wave train in front of the submerged breakwater.

The wave motion in the lee of the breakwater is shown in Fig. 7. The enevelope lines are not straight, because of the wave breaking occurring over the roof of the breakwater. Fig. 8 shows the water surface displacement, taken at four successive time instants and reveals how waves break as the pass over the roof of the breakwater.

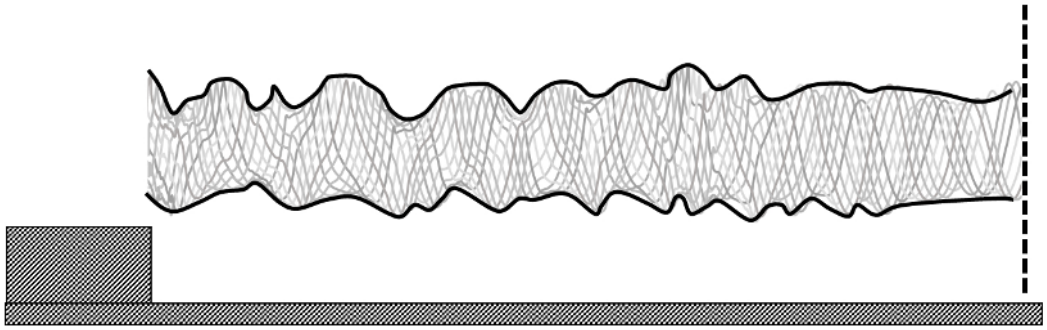

Figure 7: The wave field behind of the submerged breakwater.

Figure 8: The breaking of waves passing over the roof of the submerged breakwater.

The reflection coefficient

In Fig. 9 there is a detailed view of the wave envelope of the quasi-standing wave field of Fig 6, in which H_v and H_n are the quasi-antinode and the quasi-node height, respectively. The reflected wave height H_r, can be calculated by means of Healy's (1952) formula:

$$H_r = \frac{H_v - Hn}{2}, \tag{7}$$

H_v and H_n being equal to 1.77 m and to 1.18 m, respectively. It follows, H_r =0.30m and R = 0.2.

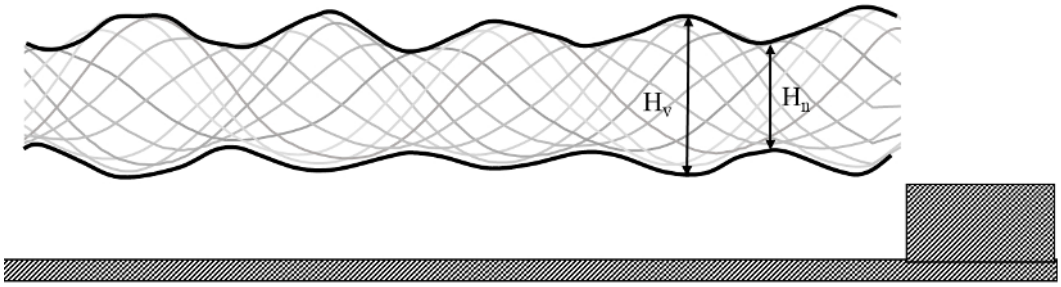

Figure 9: Wave envelope of the quasi-standing wave field in which H_v is the quasi-antinode height and H_n is the quasi-node height.

The transmission coefficient

The ratio between the height of the wave trasmitted behind the breakwater and the height of the incident waves is the transmission coefficient, T. As we can see in Fig. 10, despite the irregular shape of the envelope of the free surface displacement, the wave height remains quite constant along the channel. After a few wavelenght far from the breakwater, the wave shape tends to became more regular, assuming the classic form of progressive field formed by regular waves (see Fig.11). The average wave height is equal to 1.05 m. Therefore the transmission coefficient is equal to 0.7.

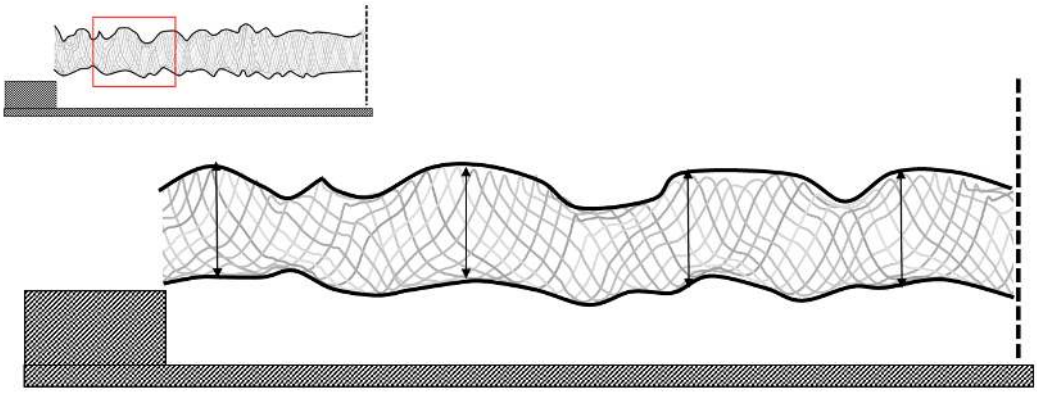

Figure 10: The wave field behind the submerged breakwater. Zoom to the first part of the envelope.

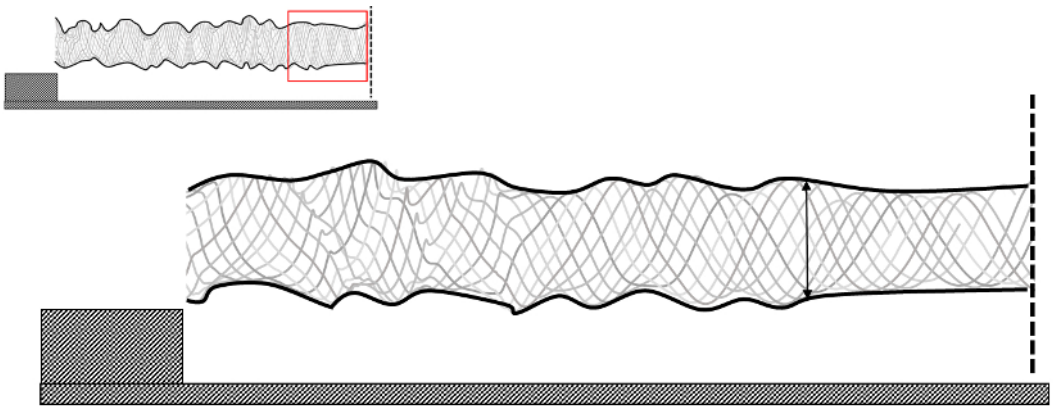

Figure 11: The wave field behind the submerged breakwater. Zoom to the last part of the envelope.

The wave energy flux and balances

To verify the share of the incident wave energy transmitted in the lee of the submerged breakwater, we calculated the energy flux Φ at different vertical sections along the wave flume. To evaluate the energy flux crossing an assigned vertical cross section we evaluate the pressure fluctuation Δp and the horizontal velocity v_y, in nearly 24 points along the vertical section. The points are taken every 0.5m, starting from the bottom, ($z = 0$) up to the free surface displacement η. The mean energy flux is evaluated as:

$$\bar{\Phi}(y) = \frac{1}{T}\int_0^T \int_0^\eta \Delta p(y,z,t) v_y(y,z,t) dz dt. \tag{8}$$

Figg. 12, 13 and 14 show the energy flux versus time at the three different abscissas shown in Fig. 15. The time span in each abscissa is chosen in order to show:

(i) in Fig. 12, the energy flux of the incoming wave train (i.e. the waves generate by the wavemaker) at section AB;

(ii) in Fig. 13, the energy flux of the wave field before the submerged breakwater, at section EF (it is a superimposition of the incoming wave field and reflected wave field);

(iii) in Fig. 14, the energy flux transmitted in the lee of the structure, at section GH.

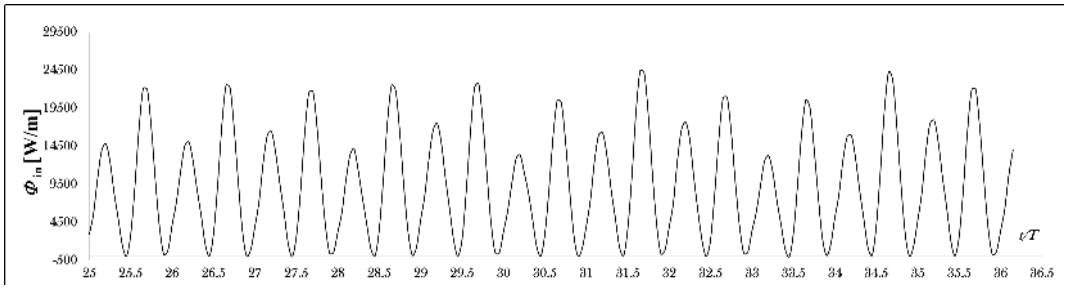

Figure 12: Energy flux of the incident waves.

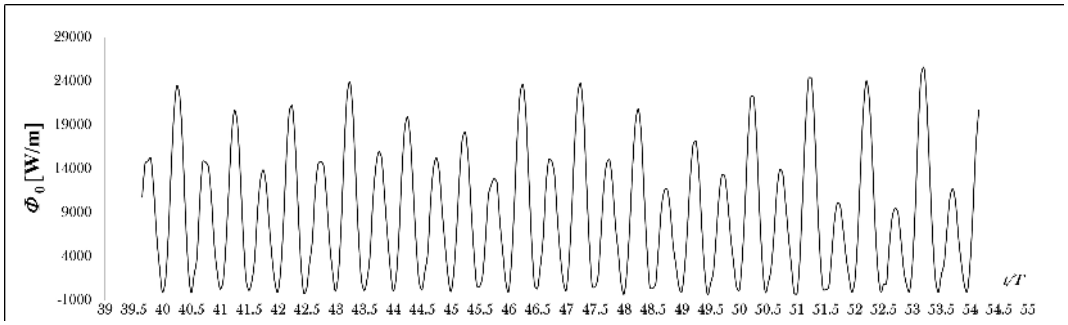

Figure 13: Energy flux of the quasi standing field in front of the submerged breakwater.

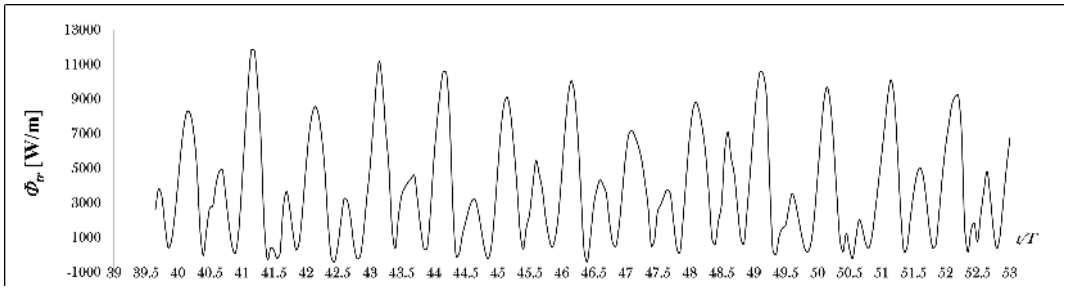

Figure 14: Energy flux behind the submerged breakwater.

In Fig. 15, three control volumes for energy balance check are shown. The mean value of the incident wave power is $\bar{\Phi}_{in}$=9.4kW/m. It is the same value obtained in section CD. This energy is partially reflected by the submerged breakwater and partially transmitted in the lee of the structure. The mean energy contained in the volume ABCD, in the time interval shown in Fig. 12, is constant because, as said, the mean energy flux crossing section CD is equal to the mean energy flux through section AB. On the contrary, the energy content of volume CDEF, during the time interval shown in Fig. 13, varies in time due to the expansion of the reflected wave field, towards the wavemaker. The energy flux $\bar{\Phi}_0$, crossing the section EF is equal to 8.7 kW/m. This is the energy flux of the quasi standing field. Finally, the flux $\bar{\Phi}_{tr}$ crossing the section GH , of the progressive waves leaving the back side of the breakwater, is equal to 3.9 kW/m. The difference $\bar{\Phi}_0$ - $\bar{\Phi}_{tr}$ = $4.8kW/m$ represents the energy dissipated by breaking over the breakwater roof.

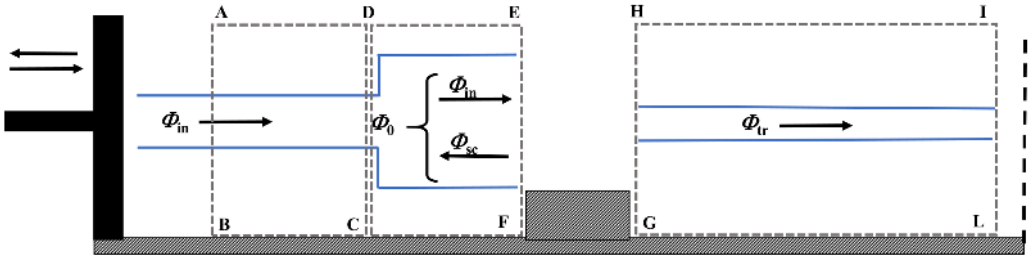

Figure 15: Control volumes for energy balance check. $\bar{\Phi}_{in}$ is the mean energy flux per unit length of the incoming waves; $\bar{\Phi}_0$ is the mean energy flux per unit length of waves before the submerged breakwater (incident + scattered), and $\bar{\Phi}_{tr}$ is the mean energy flux transmitted behind the breakwater

DISCUSSION ON NUMERICAL RESULTS: BEM VS CFD

The flow motion obtained whit BEM is ideal. Therefore, it cannot account for any energy dissipation in the field. The most relevant occurs over the breakwater roof, affecting the energy balance between reflected and trasmitted waves. In the ideal flow condition, we have

$$T^2 + R^2 = 1, \tag{9}$$

while in a dissipative medium:

$$T^2 + R^2 + L^2 = 1 \tag{10}$$

where L^2 is the wave energy lost by waves by breaking and frictions on the roof. This dissipation affects mainly the transmission of energy. It emerges clearly comparing between themselves the transmitted energy obtained with the two numerical methods:

$$T^2 = \begin{cases} 0.92 & \text{BEM,} \\ 0.41 & \text{CFD.} \end{cases}$$

As we can see, without the dissipation, the energy transmitted in the lee is 2.25 times greater. In term of transmission coefficient, this means:

$$T = \begin{cases} 0.96 & \text{BEM,} \\ 0.7 & \text{CFD.} \end{cases}$$

The wave breaking produces a significant disturbance on the shape of the transmitted waves, which need many wavelenghts of travelling distance away from the edge of the breakwater to assume a regular profile. The quasi standing wave field before the breakwater is less affected by wave breaking for what regards both the amplitude and the shape of the waves. Indeed the reflection coefficient is

$$R = \begin{cases} 0.26 & \text{BEM} \\ 0.20 & \text{CFD} \end{cases}$$

with a ratio $R_{(\text{BEM})}/R_{(\text{CFD})}$=1.3.

CONCLUSIONS

Submerged breakwaters are commonly used for coast protection. Usually, they are rubblemound breakwater with crest above or belove the mean water level. Energy dissipation on the slope and berm of submerged or low-crested breakwaters plays a fundamental role in reducing the energy transmitted in the lee.

In this work, we invistigated the wave field around a REWEC1 submerged barrier, in "non-active" configuration. In this operational condition, the barrier can be assimilated to an impermeable submerged breakwater having a rectangualre vertical section. We followed two approach: the diffraction of linear waves in the framework of potential theory; the Reynolds-averaged Navier-Stokes equations (RANS). The velocity potential of scattered waves was obtained by means of the boundary element technique. The RANS were been solved by means of the Euler- Euler approach implemented in the Ansys Fluent code, where the air-water interface was resolved through the Volume of Fluid model (VoF). The comparison among results obtained with the two different methods highlights the relevance of dissipative phenomena. They occur essentially over the roof of the breakwater, where waves break because of the abrupt reduction of the water depth. On the other hand, the wave field in front of the breakwater, obtained by means of BEM is in agreement with those obtained by CFD analysis. In front of the breakwater the wave field is a quasi-standing field, formed by the superimposition of the progressive wave moving to the breakwater and the reflective wave field moving backwards. Behind the breakwater, both the models show the existence of a progressive wave field moving away from the breakwater. However, shape and amplitude of these waves are remarkably different among them because of the dissipation.

ACKNOWLEDGEMENTS

The computing resources and the related technical support used for this work have been provided by CRESCO/ENEAGRID High Performance Computing infrastructure and its staff [G. Ponti et al., 2014]. CRESCO/ENEAGRID High Performance Computing infrastructure is funded by ENEA, the Italian National Agency for New Technologies, Energy and Sustainable Economic Development and by Italian and European research programmes, see http://www.cresco.enea.it/english for information".

REFERENCES

Ahrens JP (1987). *Characteristics of reef breakwaters.* Tech. Rep. CERC-87-17, U.S. Army Engineer Waterways Experiment Station, Vicksburg, MS.

Arena, F. & Filianoti, P. (2007) *A small-scale field experiment on a submerged breakwater for absorbing wave energy*, ASCE Journal of Waterway, Port, Coastal, and Ocean Engineering, Volume 133, Issue 2, pp. 161-167, doi:10.1061/(ASCE)0733-950X (2007)133:2(161);

Boccotti P. (2003), *On a new wave energy absorbe.* Ocean Engineering, 30, 1191-2000, 2003.

Boccotti P. (2007), *Caisson breakwaters embodying an OWC with a small opening - Part I: Theory.* Ocean Engineering, 34 (5-6), 806-819.

Boccotti P. (2007), P. Filianoti, V. Fiamma, F. Arena, *Caisson breakwaters embodying an OWC with a small opening* Engineering, 34 (5-6), 820-841.

Briganti R., JW Van der Meer, M. Buccino, M. Calabrese (2003), *Wave transmission behind low crested structures.* ASCE Proc. Coastal Structures, Portland, 580-592

Chakrabarti, S. K. 1994. *Hydrodynamics of Offshore Structures*, Southampton: Computational Mechanics Publications.

D'Angremond K, J. Van Der Meer, R. De Jong, (1996). *Wave transmission at low-crested structures.* Proceedings 25th Coastal Engineering Conference, ASCE, 2418-2427.

Filianoti P. (2015), R. Piscopo, *Sea wave energy transmission behind submerged absorber caissons.* Ocean Engineering, 93, 107-117.

G. Ponti et al.,*The role of medium size facilities in the HPC ecosystem: the case of the new CRESCO4 cluster integrated in the ENEAGRID infrastructure*, Proceedings of the 2014 International Conference on High Performance Computing and Simulation, HPCS 2014, art. no. 6903807, 1030-1033;

Healy, J.J., (1952). *Wave damping effect of beaches. Proc. Int. Hydraulics Convention*, 213-220

Seabrook S., KR Hall (1998), *Wave transmission at submerged rubble mound breakwaters.* Coastal Engineering, 2000-2013.

Wehausen, and Laitone *Surface waves* Handbuch der Physik (Ed.), S. Flugge, IX, Springer-Verlag, Berlin (1960), pp. 446-778